

STAT

Trajectory of Rays in a Magnetically  
Active Ionized Medium - Ionosphere

By: Ya. L. Al'pert

Izvestiya Akademii Nauk SSSR, Seriya Fizicheskaya, Vol XII,

No 3, Moscow, May/June 1948

pp 241-266.

STAT

TRAJECTORY OF RAYS IN A MAGNETICALLY ACTIVE IONIZED  
MEDIUM -- IONOSPHERE

Ya. L. Al'pert

(Report read at the conference of the All-Union Scientific Council on Radiophysics and Radiotechnology of the OFMN AN USSR on 13 December 1947.)

1. INTRODUCTION

The question of the trajectory both of the monochromatic wave and of the quasichromatic group of waves (signal) in a non-homogeneous anisotropic medium has not been fully analyzed up to this time.

In this article we examine the study of radio wave propagation in the ionosphere. It presents an ionized nonhomogeneous medium consisting of free electrons and it corresponds to the case of artificial anisotropy provoked by the external magnetic field of the earth.

The active magnetic properties of the ionosphere lead to the fact that the monochromatic, linear polarized, electromagnetic waves which are propagated in it are subject to double refraction. (In the case of longitudinal wave propagation, when the direction of the ray coincides with the direction of the external magnetic field vector, we have essentially the Effect of Faraday, while in the case of a transversal wave propagation, when the normal to the wave front and the external magnetic field vector are perpendicular to each other, we have the Effect of Cotton-Mouton.)

In the linearly polarized signals which constitute the group of linearly polarized monochromatic waves, both groups of waves are divided -- the signal splits into two elliptically polarized signals each one of which is subject to a different refraction and absorption in the medium. Because of this, these signals, called common and uncommon, diverge and are propagated in the ionosphere through different paths.

It is known that the ionosphere is nonhomogeneous according to the height  $z$ , and the value of the square of the refraction exponent  $n^2$  of each one of its layers diminishes with the increase of the height over the surface of the earth from a value, equalling one at the beginning of the layer, to values equalling less than zero. The value  $n^2$  depends on the degree of ionization of the layer, the wave frequency and the orientation of the external magnetic field in relation to the front of the wave. This leads to the fact that with all frequencies which are lower or nearly touching the value of the so-called critical frequency with which the layers become transparent, there occurs a complete reflection from the layer (not considering the absorption in it). Therefore, beginning from a certain height  $n^2 < 0$  for the given frequency, the further penetration of waves of this frequency into the layer ceases and all the energy of the wave falling on the layer is returned by the layer. (One must note that upon passing the critical frequency in the direction of higher frequencies, the reflection coefficient from the ionosphere drops sharply.) It is natural that each of the waves, common and uncommon, is subject to a complete reflection in different parts of the layer since they have a different value of  $n^2$  and the condition for a complete reflection  $n^2 = 0$  (1) is satisfied at various degrees of ionization (2).

The retardation of each one of the waves reflected by the layer is also different in relation to the falling wave.

In view of the fact that the approximation of geometrical optics is applicable to the analysis of radio wave propagation in the ionosphere almost up to the very point of reflection of the wave (where  $n^2 = 0$ ), one may speak of the trajectory along which the wave is propagated from the beginning of the layer to the region of its reflection and back. In other words, we may speak of its path in the ionosphere, that is, the examination of the question from the point of view of rays is fully justified. It is obvious that the question of the actual trajectory of the wave in the ionosphere and about the shape and type of the wave reflected from it offers considerable interest. At the same time, up to the present this problem has not received its due explanation in literature, mainly because of the complexity and huge volume of the theoretical calculations. Because of this a series of interesting and important facts were overlooked and not examined to their conclusion.

In the old work by Zhekulin [3] it was mentioned that the complex correlation between  $n^2$  and the angle between the direction of wave propagation and the direction of the magnetic field of the earth must lead to a rather "peculiar" trajectory of the normal to the wave front through the ionosphere (see below). However this point refers to a physically unreal case since it characterizes only the complex kinetics of the front normal of an infinite flat monochromatic wave. In practice, on the other hand, we always have to do with a limited sinusoid -- with a group of monochromatic waves, and also with a flat wave limited in space, as we may put



it with a "piece" of a flat wave, or with a spheric wave.

In a later work Booker [4] analyzed this question more thoroughly and presented a correct physical picture of the phenomenon. (It should be noted that the author became acquainted with Booker's work only after he had already completed the basic part of the present work.) Booker, however, in many respects limited himself to the general, theoretic side of the question.

In relation to the new phenomenon in the ionosphere, experimentally discovered by the author, and named "Effect of Ionosphere Anisotropy" [5], there arose the necessity to calculate the trajectory of the rays in the ionosphere. During this calculation certain theoretical difficulties were encountered. The basic difficulty however was the huge volume of the calculations in view of the necessity and desirability (and this presented an essential interest) of carrying the calculation to a numerical result, to a graph. This result could be achieved by the method of graph-analytical calculation.

This present work contains the results of these calculations and the analysis of the trajectory of the ray in the ionosphere while also examining certain characteristic peculiarities of the wave reflected from it.

## 2. TENSOR OF THE DIELECTRIC CONSTANT AND THE COEFFICIENT OF IONOSPHERE REFRACTION

Let us examine the propagation of a flat monochromatic wave

$$e^{i\omega(t - \frac{Nr}{c} - \eta)} = e^{i\varphi} \quad (2.1)$$

in an ionized medium consisting of free electrons. Here  $N(\alpha, \beta, \gamma)$  is the normal of the wave front ( $\alpha, \beta, \gamma$  are its angular coefficients, respectively the cosines of the angles  $\alpha_0, \beta_0, \gamma_0$  of the normal with the axes X, Y, Z),  $\omega$  is the angular frequency,  $t$  is the time,  $r(x, y, z)$  is the space point vector,  $s$  is the speed of light in a vacuum, and  $n$  is the refraction of the medium.

We begin with the electron movement equation

$$m \ddot{r}_0 = -e E - \frac{e}{c} [\dot{r}_0 H_0], \quad (2.2)$$

from which the member symbolizing the medium absorption has been removed and where  $m$  and  $e$  are respectively the mass and the charge of the electron (the negative sign of the electron charge has been taken into consideration);  $r_0(x_0, y_0, z_0)$  is the electron displacement vector;  $E$  is the vector of the electric field of the wave (it is assumed in (2.2) that the effective field acting on the electron is  $E_{\text{eff}} = E$ ); and  $H_0$  is the constant magnetic field of the earth.

Since the vector of the polarization of the medium volume unit is

$$P = N_0 e r_0 \text{ and } r_0 \sim e^{i\omega t},$$

where  $N_0$  is the number of electrons in one cubic centimeter, instead of (2.2) we will have

$$-P = \frac{\gamma}{4\pi} E - ih \left[ P \frac{H_0}{|H_0|} \right], \quad (2.3)$$

where

$$\gamma = \frac{4\pi N_0 e^2}{m \omega^2}, \quad h = \frac{e |H_0|}{m c \omega}. \quad (2.4)$$

The equation (2.3) introduced into the expression of the electric induction vector  $D = E + 4\pi P$ , gives

$$\left. \begin{aligned} D_x &= \left(1 - \frac{1-h_x^2}{1-h^2} v\right) E_x + \left(\frac{h_x h_y - i h_z}{1-h^2} v\right) E_y + \left(\frac{h_x h_z + i h_y}{1-h^2} v\right) E_z, \\ D_y &= \left(\frac{h_x h_y + i h_z}{1-h^2} v\right) E_x + \left(1 - \frac{1-h_y^2}{1-h^2} v\right) E_y + \left(\frac{h_y h_z - i h_x}{1-h^2} v\right) E_z, \\ D_z &= \left(\frac{h_x h_z - i h_y}{1-h^2} v\right) E_x + \left(\frac{h_y h_z + i h_x}{1-h^2} v\right) E_y + \left(1 - \frac{1-h_z^2}{1-h^2} v\right) E_z \end{aligned} \right\} (2.5)$$

and thus the tensor of the dielectric constant appears as

$$\epsilon^* = \begin{pmatrix} 1 - \frac{1-h_x^2}{1-h^2} v, & \frac{h_x h_y - i h_z}{1-h^2} v, & \frac{h_x h_z + i h_y}{1-h^2} v \\ \frac{h_x h_y + i h_z}{1-h^2} v, & 1 - \frac{1-h_y^2}{1-h^2} v, & \frac{h_y h_z - i h_x}{1-h^2} v \\ \frac{h_x h_z - i h_y}{1-h^2} v, & \frac{h_y h_z + i h_x}{1-h^2} v, & 1 - \frac{1-h_z^2}{1-h^2} v \end{pmatrix} (2.6)$$

From (2.6) it can be seen that the tensor is a hermit [isolated instance?].

In order to draw the basic formulas it is more convenient to choose the system of coordinates so that the axis Z coincides with the vector  $H_0$ . Thereby (2.5) assumes a simpler form

$$\left. \begin{aligned} D_x &= \epsilon E_x - i \epsilon_1 E_y, \\ D_y &= i \epsilon_1 E_x + \epsilon E_y, \\ D_z &= \epsilon_0 E_z, \end{aligned} \right\} (2.7)$$

where

$$\epsilon = 1 - \frac{v}{1-h^2}, \quad \epsilon_1 = \frac{h v}{1-h^2}, \quad \epsilon_0 = 1-v. (2.8)$$

Henceforth we will proceed from the phenomenological equations

\*\*\*

of Maxwell

$$c \operatorname{rot} H = \frac{\partial D}{\partial t} \quad \text{and} \quad c \operatorname{rot} E = -\frac{\partial H}{\partial t}$$

and from the wave equation deriving from it

$$\Delta E = \operatorname{grad} \operatorname{div} E + \frac{\omega^2}{c^2} D = 0,$$

which are transcribed for the flat monochromatic wave in the vector form (taking (2.1) into consideration) as

$$D = n [HN], \quad H = -n [EN] \quad (2.9)$$

and

$$D + n^2 [[EN]N] = 0 \quad \text{where} \quad D = n^2 \{E - n(EN)\}. \quad (2.10)$$

Substituting (2.7) into (2.10), we obtain the homogeneous system of equation relative to  $E_x, E_y, E_z$ :

$$\left. \begin{aligned} (n^2 - \varepsilon - n^2 \alpha^2) E_x + (-n^2 \alpha \beta + i \varepsilon_1) E_y + (n^2 - \alpha \gamma) E_z &= 0, \\ (-n^2 \alpha \beta - i \varepsilon_1) E_x + (n^2 - \varepsilon - n^2 \beta^2) E_y + (-n^2 \beta \gamma) E_z &= 0, \\ (-n^2 \alpha \gamma) E_x + (-n^2 \beta \gamma) E_y + (n^2 - \varepsilon_0 - n^2 \gamma^2) E_z &= 0 \end{aligned} \right\} (2.11)$$

The condition for the existence of a nontrivial solution for the algebraic system of equations (2.11) is that its determinant should be equal to zero:

$$\begin{vmatrix} n^2 - \varepsilon - n^2 \alpha^2, & -n^2 \alpha \beta + i \varepsilon_1, & -n^2 \alpha \gamma \\ -n^2 \alpha \beta - i \varepsilon_1, & n^2 - \varepsilon - n^2 \beta^2, & -n^2 \beta \gamma \\ -n^2 \alpha \gamma, & -n^2 \beta \gamma, & n^2 - \varepsilon_0 - n^2 \gamma^2 \end{vmatrix} = 0$$

The determinant gives a bi-square equation with respect to  $n$

$$n^4 + n^2 \frac{(\varepsilon^2 - \varepsilon_1^2 - \varepsilon \varepsilon_0) \gamma^2 - (\varepsilon^2 - \varepsilon_1^2 + \varepsilon \varepsilon_0)}{\varepsilon - (\varepsilon - \varepsilon_0) \gamma^2} + \quad (2.12)$$

$$\frac{\varepsilon_0 (\varepsilon^2 - \varepsilon_1^2)}{\varepsilon - (\varepsilon - \varepsilon_0) \gamma^2} = 0$$

from which we obtain, by utilizing (2.8) a certain formula for  $n^2$  -- the square of the exponent of ionosphere refraction:

$$n^2 = 1 - \frac{2v(1-v)}{2(1-v) - h^2(1-\gamma^2) \pm \sqrt{h^4(1-\gamma^2)^2 + 4h^2\gamma^2(1-v)^2}} \quad (2.13)$$

From the formula (2.13) follow the double refracting properties of the medium. The upper sign of the root corresponds, as is usually said, to the refraction exponent  $n_1$  for the common wave, while the lower sign corresponds to the refraction exponent  $n_2$  for the uncommon wave. An analysis of formula (2.13) shows that this terminology is not satisfactory since both waves are essentially uncommon. Figure 1 shows the relation of  $1/n_1$  and  $1/n_2$  to  $\gamma$  for various values of  $v$  and for a fixed value  $h^2 = 0.1$ . For clarity's sake we assume that for each one of the curves shown in the figure the values of  $1/n_1$  and  $1/n_2$ , when  $\gamma_0 = 0$  ( $\gamma = 1$ ), are equal to similar segments for all the values of  $v$ . Thus the curves in the figure characterize the change of the shape of the wave front with the increase of  $v$  (and consequently also of  $N_0$  (see (2.4)), i.e. with the nearing of each wave to the place of its refraction where, respectively,  $n_1 = 0$  and  $n_2 = 0$ . (See also Figures 2 and 3 where we present the family of curves  $n_1$  and  $n_2$  in relation to  $v$  for various values of  $\gamma$ .)

From Figure 1 we see that the shape of the front of each wave changes substantially upon penetrating into the layer. In the reflection sector a common wave assumes a saddlelike shape, while the uncommon one assumes a strongly stretched elliptical shape. In other words both waves cease to be spherical in the medium. The so-called common wave, one may say, has more uncommon

properties than the one that we are want to call uncommon.

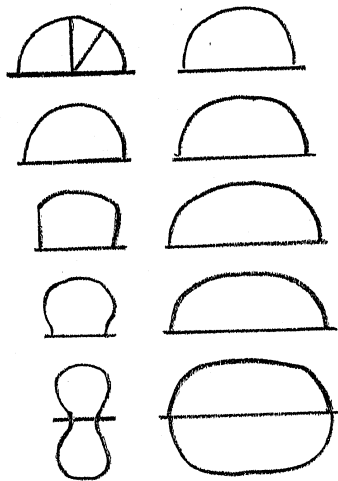


Figure 1. Relation of the quantities  $l/n_1$  and  $l/n_2$ , respectively, for a common and an uncommon wave, to  $\gamma_0$  for various values of  $v$  and for a fixed value  $h^2 = 0.1$

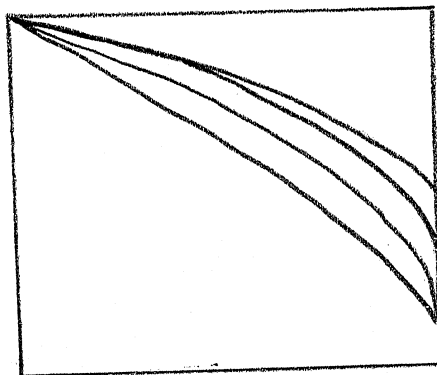


Figure 2. Relation of the refraction exponent  $n_1$  of a common wave to  $v$  with various values of  $\gamma$

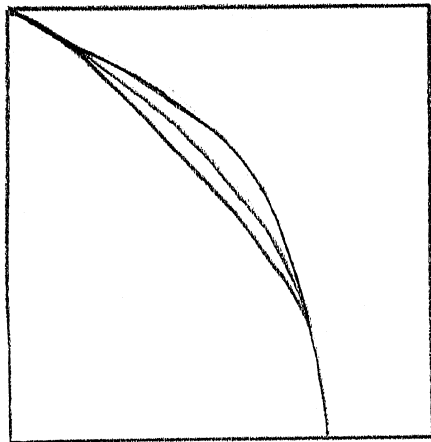


Figure 3. Relation of the refraction exponent  $n_2$  of an uncommon wave to  $v$  with various values of  $\gamma$

In order to fill out the picture let us mention a few general properties of the expression (2.13).

In the whole frequency diapason the refraction exponent  $n_1$  has but one zero which is not related to the quantity  $h$ , i.e., to the external magnetic field, and is determined from the condition (in case of  $\gamma = 1$   $n_1 = 0$  with  $v = 1 + h$ )

$$v_0 = 1 \quad (2.14)$$

This same condition is observed when the external magnetic field is absent, when  $n_1^2 = n_2^2 = 1 - v$ . The refraction exponent  $n_2$  has two zeros for  $h < 1$ , with

$$v = 1 - h \text{ and } v = 1 + h \quad (2.15)$$

For  $h > 1$ ,  $n_2$  has one zero, when  $v = 1 + h$ .



The expression  $n^2$  has infinite values for  $n_1$  in the frequency diapason  $h \cos \gamma_0 > 1$  and for  $n_2$  in the frequency diapason  $h \cos \gamma_0 < 1$  for the values of  $v$  determined by the equation

$$v = \frac{h^2 - 1}{h^2 \gamma - 1}. \quad (2.16)$$

### 3. COMPONENTS OF THE FIELD VECTOR; POLARIZATION

#### PROPERTIES OF THE WAVE

The equations (2.11) allow to determine the components with a precision up to a constant multiplier (here and later the sign  $\propto$  is used to mean "proportionate")

$$\left. \begin{aligned} E_x &\propto n^2 \gamma \{ \alpha (n^2 - \varepsilon) - i \beta \varepsilon_1 \} e^{i\varphi}, \\ E_y &\propto n^2 \gamma \{ \beta (n^2 - \varepsilon) + i \alpha \varepsilon_1 \} e^{i\varphi}, \\ E_z &\propto \{ (n^2 - \varepsilon) (n^2 \gamma^2 - \varepsilon) - \varepsilon_1^2 \} e^{i\varphi} \end{aligned} \right\} \quad (3.1)$$

where

$$\varphi = \omega \left( t - \frac{Nr}{c} \right) n.$$

From (3.1) we take the actual parts of  $E$ , indispensable in the future for the calculation of Poynting's vector:

$$\left. \begin{aligned} \text{Re } E_x &\propto n^2 \gamma \{ \alpha (n^2 - \varepsilon) \cos \varphi + \beta \varepsilon_1 \sin \varphi \}, \\ \text{Re } E_y &\propto n^2 \gamma \{ \beta (n^2 - \varepsilon) \cos \varphi - \alpha \varepsilon_1 \sin \varphi \}, \\ \text{Re } E_z &\propto \{ (n^2 \gamma^2 - \varepsilon) (n^2 - \varepsilon) - \varepsilon_1^2 \} \cos \varphi. \end{aligned} \right\} \quad (3.2)$$

Utilizing (2.9), we get from (3.1) as well as from (3.2)

$$\left. \begin{aligned} \text{Re } H_x &\propto \alpha \varepsilon_1 n^3 \gamma^2 \sin \varphi - \beta n [(n^2 - \varepsilon) \varepsilon + \varepsilon_1^2] \cos \varphi, \\ \text{Re } H_y &\propto \beta \varepsilon_1 n^3 \gamma^2 \sin \varphi + \alpha n [(n^2 - \varepsilon) \varepsilon + \varepsilon_1^2] \cos \varphi, \\ \text{Re } H_z &\propto -\varepsilon_1 n^3 \gamma (1 - \gamma^2) \sin \varphi. \end{aligned} \right\} \quad (3.3)$$

and

$$\begin{aligned} \operatorname{Re} D_x &\propto \frac{n^2 \gamma}{\varepsilon_0} \left\{ \alpha [n^2 \varepsilon - (\varepsilon^2 - \varepsilon_1^2)] \cos \varphi + \varepsilon_1 \beta n^2 \sin \varphi, \right. \\ \operatorname{Re} D_y &\propto \frac{n^2 \gamma}{\varepsilon_0} \left\{ \beta [n^2 \varepsilon - (\varepsilon^2 - \varepsilon_1^2)] \cos \varphi - \varepsilon_1 \alpha n^2 \sin \varphi \right\}, \quad (3.4) \end{aligned}$$

$$\operatorname{Re} D_z \propto \{(n^2 - \varepsilon)(n^2 \gamma^2 - \varepsilon) - \varepsilon_1^2\} \cos \varphi.$$

from the formulas (3.2) + (3.4) it follows that:

$$\left. \begin{aligned} (\operatorname{Re} H \cdot N) &= 0, & (\operatorname{Re} D \cdot N) &= 0, \\ (\operatorname{Re} E \cdot \operatorname{Re} H) &= 0, & (\operatorname{Re} D \cdot \operatorname{Re} H) &= 0, \\ (\operatorname{Re} E \cdot N) &\neq 0. \end{aligned} \right\} \quad (3.5)$$

The calculations (3.5) are for control and prove the correctness of the derived formulas since in an anisotropic medium the vector of electric induction is not collinear with the electric vector. Here we do not analyze the expression  $(\operatorname{Re} E \cdot N)$  because the following paragraph will be devoted to a detailed study of the behavior of Poynting's vector from which this question too will become clarified.

From formula (3.1) and the following we see that with an arbitrary direction of  $N$  in relation to  $H_0$  (i.e. with  $\gamma \neq 0$  and  $\gamma \neq 1$ ) both waves (for  $n_1$  and  $n_2$  respectively) are polarized along an ellipse.

In fact we get

$$\begin{aligned} E_x : E_y : E_z &= \left\{ \alpha(n^2 - \varepsilon) - i\beta\varepsilon_1 \right\} n^2 \gamma : \left\{ \beta(n^2 - \varepsilon) + i\alpha\varepsilon_1 \right\} n^2 \gamma : \\ &: \left\{ (n^2 - \varepsilon)(n^2 \gamma^2 - \varepsilon) - \varepsilon_1^2 \right\}, \quad (3.6) \end{aligned}$$

and similar expressions with imaginary members for the magnetic vector  $H$  and the vector of electric induction  $D$ .

In the case of a longitudinal propagation of the wave, when

the direction of the normal of the wave front  $N$  coincides with  $H_0$ ,  
the vector of the external magnetic field ( $\gamma = 1$ ,  $\alpha = \beta = 0$ )  
we have for both waves

$$E_z = H_z = D_z = 0$$

and, respectively for the common (index 1) and the uncommon  
(index 2) waves

$$\left. \begin{aligned} \lim_{\gamma \rightarrow 1} \left( \frac{E_x}{E_y} \right)_1 &= \frac{\epsilon_1(\alpha + i\beta)}{\epsilon_1(\beta - i\alpha)} = +i, & \left( \frac{H_x}{H_z} \right)_1 &= +i, & \left( \frac{D_x}{D_y} \right)_1 &= -i, \\ \lim_{\gamma \rightarrow 1} \left( \frac{E_x}{E_y} \right)_2 &= -i, & \left( \frac{H_x}{H_z} \right)_2 &= -i, & \left( \frac{D_x}{D_y} \right)_2 &= +i \end{aligned} \right\} (3.7)$$

i.e. all the vectors of the field are polarized along a circle  
and the common wave is polarized to the left, while the uncommon  
wave is polarized to the right. (A detailed analysis of (3.6)  
shows that a similar difference in the rotation direction is found  
also in the general case of an elliptical polarization of the wave.)

On the other hand, in the case of a transverse propagation  
of the wave, when  $\gamma = 0$

$$\left. \begin{aligned} E_{z1} &\neq 0, & E_{x1} &= E_{y1} = 0, \\ H_{z1} &= 0, & H_{x1} &\neq 0, & H_{y1} &= 0, \\ D_{z1} &\neq 0, & D_{x1} &= D_{y1} = 0 \end{aligned} \right\} (3.8)$$

i.e. all the vectors of the common wave are polarized in linear  
fashion. This however does not happen for the uncommon wave. For  
it

$$\left. \begin{aligned} H_{z2} &\neq 0, & H_{x2} &= H_{y2} = 0, \\ D_{z2} &= 0, & D_{x2} &\neq 0, & D_{y2} &\neq 0 \end{aligned} \right\} (3.9)$$

$$E_{z2} = 0, \lim_{\gamma \rightarrow 0} \left( \frac{E_x}{E_{y2}} \right) = \frac{\alpha \beta_1 + i \beta \epsilon}{\beta \epsilon - i \alpha \epsilon}, \quad (3.10)$$

i.e. the vectors D and H are polarized in linear fashion while the electric vector is polarized along an ellipse. (In writing (3.7) + (3.10) we utilized the limit correlations issuing from (2.12):

$$\eta_{1,2}^2 = \epsilon \pm \epsilon, \text{ when } \gamma = 1 \text{ AND } \eta_1^2 = \epsilon_0 \text{ AND } \eta_2^2 = \frac{\epsilon^2 - \epsilon_1^2}{\epsilon} \text{ when } \gamma = 0$$

The properties of the uncommon wave with  $\gamma = 0$  may at first sight seem strange because of their unusualness. In the following paragraph, however, with the study of Pointing's vector this result will become understandable.

#### 4. STUDY OF POINTING'S VECTOR

It is known that in nongyrotropic anisotropic media the direction of propagation of the ray coincides with the direction of Pointing's vector which characterizes the energy flow. In magnetically active media, however, (and in the ionosphere in particular) in order to clarify the question of the direction of ray propagation it is essential to make a special analysis of the character of change in Pointing's vector and to establish the correlation between it and the direction of the ray. This and the following paragraphs will be devoted to the analysis of this question.

With a precision down to a constant multiplier Pointing's vector is

$$S \approx (\text{Re } E \cdot \text{Re } H).$$

Utilizing (3.2) and (3.3) we obtain

$$\left. \begin{aligned}
 S_x &\approx n^2 \gamma^2 \alpha \epsilon_1^2 (1-\gamma^2) \sin^2 \varphi - n^3 \gamma^2 \beta \epsilon_1 \{(\eta^2 - \epsilon)^2 - \epsilon_1^2\} \sin \varphi \cos \varphi - \\
 &\quad - n \alpha \{\epsilon(\eta^2 - \epsilon) + \epsilon_1^2\} \{(\eta^2 - \epsilon)(\eta^2 - \epsilon) - \epsilon_1^2\} \cos^2 \varphi, \\
 S_y &\approx n^2 \gamma^2 \beta \epsilon_1^2 (1-\gamma^2) \sin^2 \varphi + n^3 \gamma^2 \alpha \epsilon_1 \{(\eta^2 - \epsilon)^2 - \epsilon_1^2\} \sin \varphi \cos \varphi - \\
 &\quad - n \beta \{\epsilon(\eta^2 - \epsilon) + \epsilon_1^2\} \{(\eta^2 - \epsilon)(\eta^2 - \epsilon) - \epsilon_1^2\} \cos^2 \varphi \\
 S_z &\approx n^2 \gamma^3 \epsilon_1^2 (1-\gamma^2) \sin^2 \varphi + n^3 \gamma (1-\gamma^2) (\eta^2 - \epsilon) \{\epsilon(\eta^2 - \epsilon) + \epsilon_1^2\} \cos^2 \varphi.
 \end{aligned} \right\} (4.1)$$

Let us further say that  $\alpha = 0$  (i.e.  $\beta^2 = 1 - \gamma^2$ ). This does not destroy the generality and makes the analysis of the change of S more convenient. In this case the expressions (4.1) are transcribed as

$$\left. \begin{aligned}
 S_x &\approx -n^3 \gamma^2 \beta \epsilon_1 \{(\eta^2 - \epsilon)^2 - \epsilon_1^2\} \sin \varphi \cos \varphi, \\
 S_y &\approx n^2 \gamma^2 \beta \epsilon_1^2 (1-\gamma^2) \sin^2 \varphi - \\
 &\quad - n \beta \{\epsilon(\eta^2 - \epsilon) + \epsilon_1^2\} \{(\eta^2 - \epsilon)(\eta^2 - \epsilon) - \epsilon_1^2\} \cos^2 \varphi \\
 S_z &\approx n^2 \gamma^3 \epsilon_1^2 (1-\gamma^2) \sin^2 \varphi + n^3 \gamma (1-\gamma^2) (\eta^2 - \epsilon) \{\epsilon_1^2\} \cos^2 \varphi.
 \end{aligned} \right\} (4.2)$$

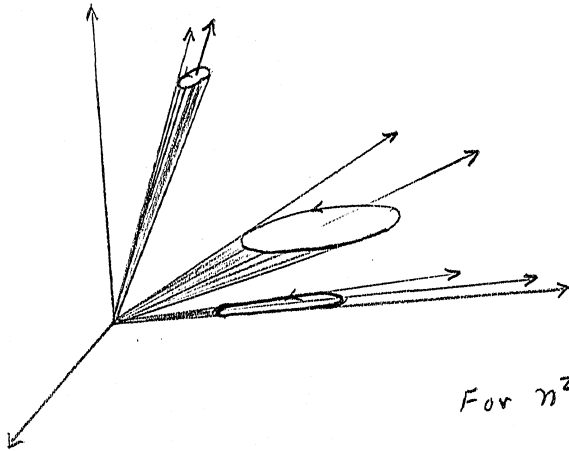
Figure 4 shows the change of position of Pointing's vector S in the space of common ( $n_1$ ) and uncommon ( $n_2$ ) waves with various values of  $\gamma_0$ , the angle between the normal N to the wave front and the vector of the external magnetic field  $H_0$ . From Figure 4 we see that S delineates a cone which touches the vector N. During one period the vector S makes two revolutions around the base. The base of the cone, consisting of a flat curve of elliptical shape, is placed symmetrically in relation to the plane ( $H_0 N$ ) which divides the cone into two equal halves. With a decrease of the angle  $\gamma_0$

the cone is flattened (the angle  $\gamma$  of its apex is reduced) and finally is reduced to a straight line when  $\gamma_0 = 0$ , i.e., with a longitudinal propagation of the wave the direction of  $S$  is constant. When  $\gamma_0 \rightarrow \frac{\pi}{2}$  for the common wave, the base of the cone is flattened so that its components  $S_x$  and  $S_y$  diminish, while for  $\gamma_0 = \frac{\pi}{2}$  (transverse propagation) the direction of  $S$  is constant and coincides with the axis  $Y$  (direction of  $N$ ). For the uncommon wave, on the other hand, in this limiting case the cone is reduced to a flat curve so that its base lies on the plane  $(XY)$ , touching the axis  $X$ . Thereupon, because of the symmetry of this curve in relation to the axis  $Y$ , the direction of  $\bar{S}$  coincides with the axis  $Y$ , i.e. with the direction of  $N$ . The vectors  $S$  of a common and of an uncommon wave also differ in that the cone formed by the vector  $S$  of a common wave touches  $N$  in the interval of transformation  $\gamma_0 = 0 + \frac{\pi}{2}$  from the external side, i.e., it is placed outside of the angle  $(H_0N)$ , while for an uncommon wave it is placed inside the angle  $(H_0N)$  (see Figure 4); the opposite position of the cone happens in the transformation interval  $\gamma_0 = \frac{\pi}{2} + \pi$  where the cone of the common wave is placed inside the angle  $(H_0N)$  and that of the uncommon wave outside of that angle.

The direction of Pointing's vector, averaged according to time, as can easily be shown, coincides with the direction of the vector traced from the apex of the cone through the center of its base and lying on the plane  $(H_0N)$ . In Figure 4 this vector is named  $\bar{S}$  (the line indicates the averaging according to time).



For  $n'$



For  $n''$

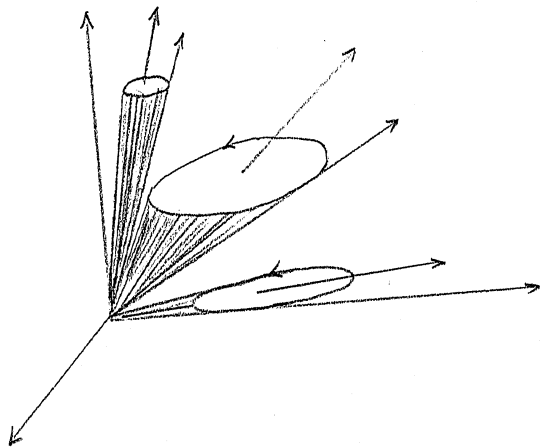


Figure 4. Change of position of Point's vector  $S$  in the space of a common ( $n_1$ ) wave and of an uncommon ( $n_2$ ) wave according to time for various values of  $\gamma_0$



The averaging of S according to time gives

$$\begin{aligned} \bar{S}_x &= 0, \\ S_y &\approx \frac{1}{2} \left\{ n^5 \gamma^2 \beta \varepsilon_1^2 (1-\gamma^2) - n \beta [\varepsilon(n^2-\varepsilon) + \varepsilon_1^2] [(n^2-\varepsilon)(n^2\gamma^2-\varepsilon) - \varepsilon_1^2] \right\} \\ S_z &\approx \frac{1}{2} \left\{ n^5 \gamma^3 \varepsilon_1^2 (1-\gamma^2) + n^2 \gamma (1-\gamma^2) (n^2-\varepsilon) [\varepsilon(n^2-\varepsilon) + \varepsilon_1^2] \right\}, \end{aligned} \quad (4.3)$$

from where, by calling the angle between  $H_0$  and  $\bar{S}$   $\psi$ , we get

$$\tan \psi = \tan \gamma \frac{n^4 \gamma^2 \varepsilon_1^2 (1-\gamma^2) - [\varepsilon(n^2-\varepsilon) + \varepsilon_1^2] [(n^2-\varepsilon)(n^2\gamma^2-\varepsilon) - \varepsilon_1^2]}{n^4 \gamma^2 \varepsilon_1^2 (1-\gamma^2) + n^2 (1-\gamma^2) (n^2-\varepsilon) [\varepsilon(n^2-\varepsilon) + \varepsilon_1^2]} \quad (4.4)$$

Figures 5 and 6 give the families of curves with the values of the angle  $\psi_0$  between  $\bar{S}$  and N equal to

$$\psi_0 = \gamma_0 - \psi, \quad (4.5)$$

These values have been computed with the help of formulas (4.4), respectively, for the common and uncommon waves ( $n_1$  and  $n_2$ ) in relation to  $\gamma_0$  for constant values of  $v$  and  $h^2 = 0.1$ . We will utilize these curves later in calculating the ray trajectory in the ionosphere.

From the figures we see that with certain values of  $v$  and  $\gamma$  the direction of the vector  $\bar{S}$  differs considerably from that of N.

The averaging of  $S$  according to time gives

$$\begin{aligned} \bar{S}_x &= 0, \\ S_y &\approx \frac{1}{2} \left\{ n^2 \gamma^2 \beta \varepsilon_1^2 (1-\gamma^2) - n \beta [\varepsilon_1 (n^2 - \varepsilon) + \varepsilon_1^2] [(n^2 - \varepsilon)(n^2 \gamma^2 - \varepsilon) - \varepsilon_1^2] \right\} \\ S_z &\approx \frac{1}{2} \left\{ n^2 \gamma^3 \varepsilon_1^2 (1-\gamma^2) + n^2 \gamma (1-\gamma^2) (n^2 - \varepsilon) [\varepsilon_1 (n^2 - \varepsilon) + \varepsilon_1^2] \right\}, \end{aligned} \quad (4.3)$$

from where, by calling the angle between  $H_0$  and  $\bar{S}$   $\psi$ , we get

$$\tan \psi = \tan \gamma \frac{n^2 \gamma^2 \varepsilon_1^2 (1-\gamma^2) - [\varepsilon_1 (n^2 - \varepsilon) + \varepsilon_1^2] [(n^2 - \varepsilon)(n^2 \gamma^2 - \varepsilon) - \varepsilon_1^2]}{n^2 \gamma^2 \varepsilon_1^2 (1-\gamma^2) + n^2 (1-\gamma^2) (n^2 - \varepsilon) [\varepsilon_1 (n^2 - \varepsilon) + \varepsilon_1^2]} \quad (4.4)$$

Figures 5 and 6 give the families of curves with the values of the angle  $\psi_0$  between  $\bar{S}$  and  $N$  equal to

$$\psi_0 = \gamma_0 - \psi, \quad (4.5)$$

These values have been computed with the help of formulas (4.4), respectively, for the common and uncommon waves ( $n_1$  and  $n_2$ ) in relation to  $\gamma_0$  for constant values of  $v$  and  $h^2 = 0.1$ . We will utilize these curves later in calculating the ray trajectory in the ionosphere.

From the figures we see that with certain values of  $v$  and  $\gamma$  the direction of the vector  $\bar{S}$  differs considerably from that of  $N$ .

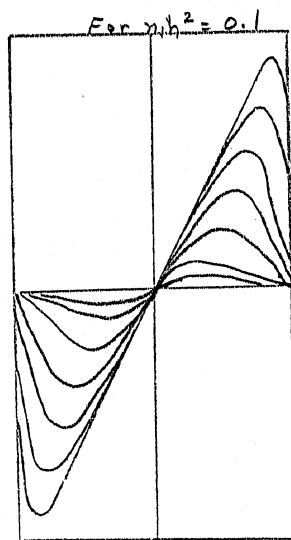


Figure 5. Family of curves expressing the relation of the angle  $\psi_0$  to the angle  $\gamma_0$  between  $H_0$  and  $N$  for various values of  $v$  when  $h^2=0.1$  for common wave ( $n_1$ )

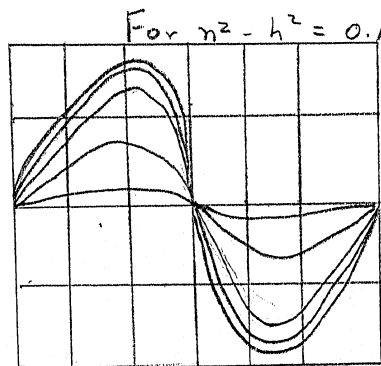


Figure 6. Same as in Figure 5 for an uncommon wave ( $n_2$ )

## 5. DIRECTION AND MAGNITUDE OF GROUP SPEED

In practice we always have to deal not with a monochromatic wave, but with a signal, or group of monochromatic waves. Therefore in order to find the direction of the signal we must examine the propagation of the quasi-monochromatic group of waves, presenting the components of all the signal field vectors in the form of Fourier's integral

$$U(r, t) = \iiint g(k) e^{i(\omega t - kr)} dk_x dk_y dk_z \quad (5.1)$$

In the integral (5.1)  $g(k)$  is the function characterizing the shape of the signal. It has, as we know, a sharp maximum in the vicinity of  $k$ . The wave vector for anisotropic media has in the general case the form

$$K = \frac{\omega}{c} n\left(\omega, \frac{k_x}{K}, \frac{k_y}{K}, \frac{k_z}{K}\right) \frac{K}{K}, \quad (5.2)$$

or, with the specifications given above:

$$\left. \begin{aligned} K &= \frac{\omega}{c} n(\omega, \alpha, \beta, \gamma) \\ K &= \sqrt{k_x^2 + k_y^2 + k_z^2}, \quad l = \alpha^2 + \beta^2 + \gamma^2, \\ K_x &= \alpha \cdot K, \quad K_y = \beta \cdot K, \quad K_z = \gamma \cdot K. \end{aligned} \right\} \quad (5.3)$$

Choosing, just as we did in Section 2, the direction of the axis Z along the vector of the external magnetic field  $H_0$  and utilizing for  $n$  the expression which is written in as a function of the angular coefficient  $\gamma$  (see (2.13)) we get:

$$K = \frac{\omega}{c} n(\omega, \gamma) N. \quad (5.4)$$

We resolve, as usual, the integral (5.1) in the vicinity of  $k_0$  (the fixed frequency  $\omega_0$ ). Limiting ourselves to the first two members of the resolution

$$\omega = \omega_0 + \left( \frac{\partial \omega}{\partial k_x} \Delta k_x + \frac{\partial \omega}{\partial k_y} \Delta k_y + \frac{\partial \omega}{\partial k_z} \Delta k_z \right) + \dots,$$

we get

$$u(r, t) = e^{i(\omega_0 t - k_0 r)} \iiint g(k) e^{i \left( \frac{\partial \omega}{\partial k} \Delta k \cdot r - \Delta k \cdot r \right)} dk_x dk_y dk_z, \quad (5.5)$$

where

$$\frac{\partial \omega}{\partial k} = \frac{\partial \omega}{\partial k_x} x_0 + \frac{\partial \omega}{\partial k_y} y_0 + \frac{\partial \omega}{\partial k_z} z_0$$

$$\Delta k = \Delta k_x x_0 + \Delta k_y y_0 + \Delta k_z z_0$$

and  $x_0, y_0, z_0$  are respectively the unit vectors of the coordinate system axes.

From (5.5) we get by the usual way the vector of group speed of the quasi-monochromatic group of waves (signal)

$$U = \frac{\partial \omega}{\partial k}, \quad (5.6)$$

which determines the measure of the group speed and the direction of propagation of the quasi-monochromatic group of waves.

The corresponding calculations give us

$$\frac{\partial \omega}{\partial k_x} = \frac{\alpha \frac{\partial(n\gamma)}{\partial \gamma}}{\frac{h}{c} \cdot \frac{\partial(\omega n)}{\partial \omega}}, \quad \frac{\partial \omega}{\partial k_y} = \frac{\beta \frac{\partial(n\gamma)}{\partial \gamma}}{\frac{h}{c} \cdot \frac{\partial(\omega n)}{\partial \omega}}, \quad \frac{\partial \omega}{\partial k_z} = \gamma \frac{\left[ \frac{\partial(n\gamma)}{\partial \gamma} - \frac{1}{\gamma} \cdot \frac{\partial n}{\partial \gamma} \right]}{\frac{h}{c} \cdot \frac{\partial(\omega n)}{\partial \omega}} \quad (5.7)$$

from where it follows that the magnitude of the group speed is equal to

$$U = \left| \frac{d\omega}{dk} \right| = \sqrt{\frac{1 + \frac{1-\gamma^2}{n^2} \left( \frac{\partial n}{\partial \gamma} \right)^2}{\frac{1}{c} \cdot \frac{\partial(\omega n)}{\partial \omega}}}. \quad (5.8)$$

The angle between the vector of the group speed  $U$ , which characterizes the signal propagation direction, and the normal to the wave front  $N$  is determined from the formula

$$\frac{(UN)}{U} = \cos(NU) = \frac{1}{\sqrt{1 + \frac{1-\gamma^2}{n^2} \left( \frac{\partial n}{\partial \gamma} \right)^2}}. \quad (5.9)$$

Further on we will also need the angle between the axis  $Z$  and  $U$ . For  $\alpha = 0$ , from (5.7) follows

$$\tan(UZ_0) = \frac{\frac{\partial \omega}{\partial k_y}}{\frac{\partial \omega}{\partial k_z}} = \frac{\beta}{\gamma} \cdot \frac{\frac{\partial(n\gamma)}{\partial \gamma}}{\frac{\partial(n\gamma)}{\partial \gamma} - \frac{1}{\gamma} \cdot \frac{\partial n}{\partial \gamma}}, \quad (5.10)$$

or, substituting

$$\frac{\partial n}{\partial \gamma} = \frac{n(1-n^2)^2 \gamma h^2}{2(1-\nu)(\nu-1+n^2) + (1-n^2)(1-\gamma^2) h^2} \quad (5.11)$$

which we have determined from (2.13) we transcribe (5.10) in a way



more convenient for calculation

$$c \tan(UZ_0) = c \tan \gamma \left\{ 1 - \frac{1}{\gamma^2 + \frac{1-\gamma^2}{1-n^2} - \frac{2(1-v)(1-v-n^2)}{(1-n^2)^2 h^2}} \right\} \quad (5.12)$$

If  $\frac{dn}{d\gamma} = 0$ , which occurs in an isotropic medium, then from the formulas (5.8) and (5.9) it follows that

$$U_0 = \frac{c}{\frac{\partial(\omega n)}{\partial \omega}}$$

and also that U and N are parallel.

Figures 7 and 8 show families of curves for the relation between the magnitude of the signal group speed  $U_0$  propagating in an isotropic medium and the magnitude of the signal speed U in a magnetically active medium formula (5.8) in relation to  $\gamma$  for various values of  $v$  with  $h^2 = 0.1$ , respectively, for common ( $n_1$ ) and uncommon ( $n_2$ ) waves. From the figures we see that under certain conditions U differs from  $U_0$  to a significant extent.

It should be mentioned that the necessity to apply formulas (5.8) and (5.9) in calculating the propagation of radio waves in the ionosphere has not heretofore been mentioned in literature. In a number of works the formula for the isotropic medium was erroneously applied when making these calculations. Further on, however, we will show that the group path of the signal in the ionosphere may be calculated after a formula analogous to that for the isotropic medium. Because of that, in certain cases, correct results were still obtained with the help of incorrect formulas [6].



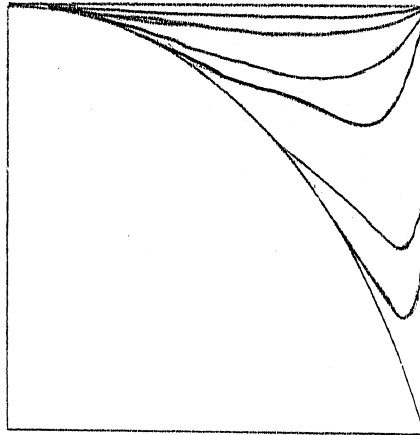


Figure 7. Family of curves expressing the relation between the ratio magnitude of the signal group speed  $U_0$  in an isotropic medium to magnitude of signal group speed  $U$  in a magnetically active medium and  $\gamma_{H_0 N}$  for various values of  $\nu$  with  $h^2 = 0.1$ .  
(Common wave  $n_1$ )

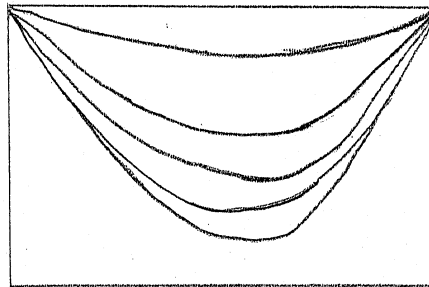


Figure 8. Same as in Figure 7, but for an uncommon wave ( $n_2$ )

The calculation of the signal direction in the ionosphere, made in this paragraph and leading to the formulas (5.10) and (5.12) allows us to control whether the direction of the vector  $\vec{S}$  and the direction of the signal propagation coincide. In practice this means checking the sameness of formulas (5.10) and (4.4). Comparing these we get the expression

$$\begin{aligned} & \{n^6(1-h^2-v)(1-h^2) - n^4[(1-h^2)((1-v)^2-h^2) + 2(1-v-h^2)^2] + \\ & + n^2\{[(1-v)^2-h^2](1-h^2-v) - [(1-v)^2-h^2]\} : \{n^6(1-h^2-v)(1-h^2)\gamma^2 - \\ & - n^4[(1-n^2)((1-v)^2-h^2)\gamma^2 + ((1+\gamma^2)(1-v-h^2)^2) - \gamma^2 h^2 v^2 (1-\gamma^2)] + \\ & + n^2[(1-v)^2-h^2](1-v-h^2)(2+\gamma^2) - [(1-v)^2-h^2]\} = \\ & = (n^2-v)^2 h^2 : \{n^4 \gamma^2 h^2 + n^2(2-h^2-2v-\gamma^2 h^2) + (-2+h^2+4v-2v^2)\}, \quad (5.13) \end{aligned}$$

which is reduced to a polynome of the eighth degree in relation to  $n$ . We introduce  $n^2$  into (5.13) (see (2.13)) after which it may be transcribed as

$$\begin{aligned} [n^4] = n^4(1-h^2-v+h^2v\gamma^2) + n^2(-2+2h^2+4v-vh^2-2v^2h^2\gamma^2v) + \\ + (1-3v-h^2+vh^2+3v^2-v^3) = 0 \quad (5.14) \end{aligned}$$

This leads us to the expression

$$2[n^4]^2 - [n^4] \cdot n^2(vh^2-3vh^2\gamma^2) - [n^4] \cdot n^4(vh^2-\gamma^2) \equiv 0, \quad (5.15)$$

which, as we see, is equal to zero. This proves that  $\vec{S} \parallel \vec{U}$ .

(Recently S. M. Rytov has proven this theorem in its general aspect [7]).

In conclusion of this section it is useful to dwell on certain properties of the signal, arising out of the analysis of the formulas developed above.

From physical considerations it is obvious that in the case of a homogeneous medium the time of group retardation of the signal

is equal to

$$t_{gr} = \frac{\sqrt{x^2 + y^2 + z^2}}{u} = \frac{x}{\frac{\partial \omega}{\partial k_x}} = \frac{y}{\frac{\partial \omega}{\partial k_y}} = \frac{z}{\frac{\partial \omega}{\partial k_z}}, \quad (5.16)$$

whence, by way of simple transformations, we get

$$t_{gr} = \frac{ax + \beta y + \gamma z}{a \frac{\partial \omega}{\partial k_x} + \beta \frac{\partial \omega}{\partial k_y} + \gamma \frac{\partial \omega}{\partial k_z}} \quad (5.17)$$

Since (5.7) gives

$$a \frac{\partial \omega}{\partial k_x} + \beta \frac{\partial \omega}{\partial k_y} + \gamma \frac{\partial \omega}{\partial k_z} = \frac{1}{c \cdot \frac{\partial(\omega n)}{\partial \omega}},$$

we get

$$t_{gr} = \frac{1}{c} \cdot \frac{\partial(\omega n)}{\partial \omega} (ax + \beta y + \gamma z). \quad (5.18)$$

In the case of a nonhomogeneous medium the time of group retardation of the signal, in the approximation of geometric optics, is equal to

$$t_{gr} = \int \frac{ds}{u} = \int \frac{dl}{u \cos(Nu)} = \int \frac{dl}{u_0}, \quad (5.19)$$

where  $ds$  is the element of length in the direction of the signal  $U$  propagation; and  $dl$  is the element of length in the direction of the normal to the wave front  $N$ . In (5.19) we have

$$\frac{u_e}{u} = \cos(NU),$$

which follows from (5.8) and (5.9).

The expressions obtained -- (5.18) and (5.19) -- show that the formulas determining  $t_{gr}$  are identical to the known formulas for the isotropic medium.

$$\alpha' \frac{d\omega}{dk_x} + \beta' \frac{d\omega}{dk_y} + \gamma' \frac{d\omega}{dk_z} = 0 \quad (5.20)$$

will be the condition for the reflection of the signal in a stratified nonhomogeneous medium. This condition, within the approximation of geometrical optics, means that at the point of reflection the tangent to the trajectory of the ray must be horizontal. Here  $\alpha', \beta', \gamma'$  are respectively the cosines of the angles between the axis  $Z$  (along  $H_0$ ) and the direction of  $Z'$ , along which the medium is nonhomogeneous in layers.

From (5.20) we get

$$n = \frac{\partial n}{\partial \gamma'} \left( \frac{\gamma' - \cos(NZ')}{\cos(NZ')} \right). \quad (5.21)$$

(Upon vertical descent on the layer the reflection condition  $n = 0$  is general.)

It must be remembered that in formula (5.21)  $\gamma' = \cos(NH_0)$  is the cosine of the angle between the normal to the wave front  $N$

and the vector of the external magnetic field  $H_0$ .

The signal reflection condition in a magnetically active medium thus obtained differs from that in an isotropic medium, where at the point of reflection

$$n = \sin \chi_0, \quad \cos(NZ_0) = 0,$$

where  $\chi$  is the angle between the normal and the Z axis at the beginning of the layer, i.e. is the angle of descent. (The calculation of the values of  $v$  from (5.21) at the point of reflection is very cumbersome. However, one may utilize the graphic method to solve this equation which, upon utilization of additional conditions relating  $v$  and  $\chi$  (see (6.4) and (6.5)), permits construction of a chart for  $v_0(\sin \chi_0)$  which will determine the value of ionization of the layer at the point of reflection in relation to the angle  $\chi_0$  of wave descent upon the layer.)

#### 6. METHOD OF CALCULATING THE TRAJECTORY OF THE RAY

In the preceding sections we obtained formulas which allowed us to calculate within an approximation of geometrical optics the trajectory of signal propagation in a nonhomogeneous, magnetically active medium. Because of their complexity they are solved only by way of combining graphic and analytical calculations. This provides satisfactory precision for the drawing of the whole picture both from the qualitative and the quantitative points of view.

Let us assume that at the beginning of a layer along the Z axis the normal of the descending wave forms with the Z axis an angle  $\chi_0$  and lays on the plane XZ which thereby becomes the plane of wave descent. Let us choose the system of coordinates shown in

Figure 9. With the specifications assumed before, the vectors which interest us are inscribed as

$$H_0 = H_0(\alpha_H, \beta_H, \gamma_H),$$

$$N = N(\alpha, 0, \gamma),$$

$$U = U(\alpha_1, \beta_1, \gamma_1).$$

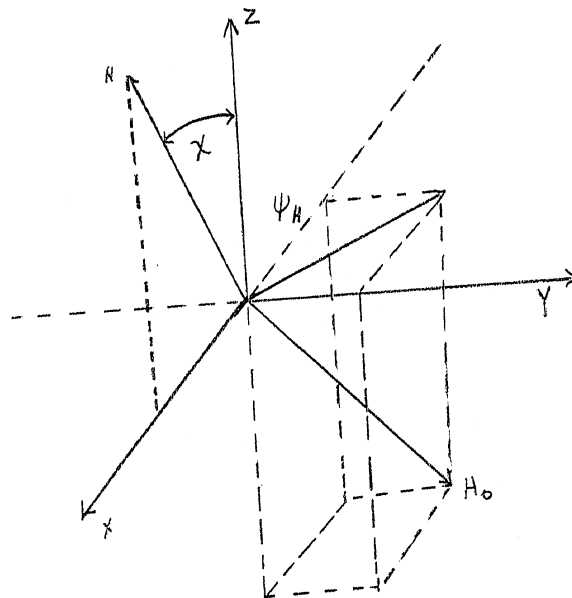


Figure 9

Because of the law of Snellius (see the general theory of anisotropic media in optics text books) the normal to the front of waves of different types remains everywhere parallel to the plane of wave descent.

We are interested in calculating the values of angular coefficients  $\alpha_1, \beta_1, \gamma_1$  of the group speed vector  $U$  along the

whole propagation path of both waves, from the beginning of the layer to the point of reflection and back, i.e., in the interval of  $v$  values from  $v = 0$  (beginning of the layer, see Section 2) to those values of  $v$  at which the reflection of each wave takes place. The values of  $\alpha_1(v)$ ,  $\beta_1(v)$ ,  $\gamma_1(v)$  are determined by the system of equations

$$\begin{vmatrix} \alpha_1 & \beta_1 & \gamma_1 \\ \alpha_H & \beta_H & \gamma_H \\ \alpha & 0 & \gamma \end{vmatrix} = 0, \quad (6.1)$$

$$\alpha_1 \alpha + \gamma_1 \gamma = \cos(NU) = \cos \psi_0, \quad (6.2)$$

and

$$\alpha_1^2 + \beta_1^2 + \gamma_1^2 = 1. \quad (6.3)$$

The expression (6.1) shows that the vector of group speed  $U$  (and also the vector  $\bar{S}$ , see Section 4) lies always on the plane  $(NH_0)$ . The expression (6.2) determines the angle between  $N$  and  $U$  (see Figures 5 and 6), while (6.3) is the known condition connecting the angular coefficients of the straight line.

If in the given interval of  $v$  values we know the values of  $\alpha$ ,  $\gamma$  and  $\cos \psi$  ( $\alpha_H, \beta_H$  and  $\gamma_H$  are assumed to be constant), then from (6.1) - (6.3) we may determine the totality of values needed to build the functions  $\alpha_1(v)$ ,  $\beta_1(v)$ ,  $\gamma_1(v)$ .

The values of  $\psi_0$  for the interval of  $v$  in the function of the angle between the normal  $N$  and  $H_0$  ( $\sqrt{H_0 N} = \cos H_0 N$ ) are cal-



culated and presented in Figures 5 and 6. As for the values of  $\alpha(v)$  and  $\gamma(v)$ , they are determined from the equations

$$\alpha \cdot n(v, \gamma H_0 N) = \sin \chi_0 \quad (6.4)$$

(law of Snellius), and

$$\gamma H_0 N = \alpha_H \alpha + \gamma_H \gamma, \quad (6.5)$$

where  $\alpha(v) = \sin \chi$ ,  $\gamma(v) = \cos \chi$ , and  $\chi$  is the angle between N and the Z axis (see Figure 9). The determination of  $\alpha(v)$  and  $\gamma(v)$ , or, to make further calculations easier, the determination of the function  $\chi(v)$ , is best achieved by way of a graph with the intersection of the family of curves

$$\chi = \arcsin \left( \frac{\sin \chi_0}{n(\chi, \gamma H_0 N)} \right) \quad \text{when } v = \text{const.} \quad (6.6)$$

and

$$\chi = \arcsin \left\{ \frac{-\alpha_H \gamma \pm \sqrt{(\alpha_H \gamma H_0 N)^2 + (\gamma_H^2 - \gamma_{H_0 N}^2)(\alpha_H^2 + \gamma_H^2)}}{\alpha_H^2 + \gamma_H^2} \right\} \quad (6.7)$$

obtained from (6.5). This is so because of the complexity of the expression  $n(v, \sin \chi \alpha_H + \cos \chi \gamma_H)$  (see (2.13)).

Figure 10 shows the respective families of curves for  $n_1$  (with  $\chi_0 = 5^\circ$ ), while Figure 11 shows the same for  $n_2$ . (A large number of graphs in the interval  $\chi_0 = 2 + 26^\circ$  was needed for a detailed analysis. Here we render only a small part of the total.)

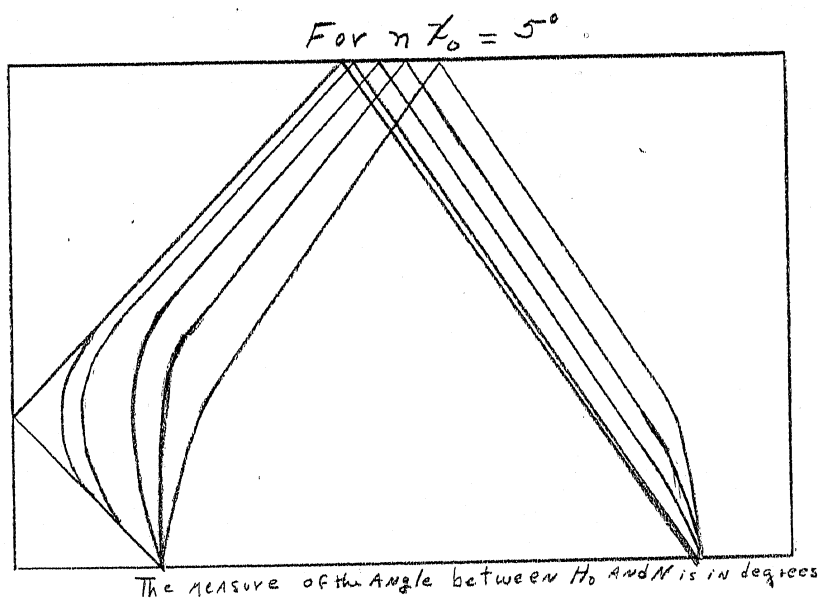


Figure 10. Family of curves of the quantity  $\chi$ , calculated according to formula (6.6). Dotted lines are for the fixed values of  $\nu$  and according to the formula (6.7). Black lines are for the fixed values of  $\alpha_H$  and  $\gamma_H = 0.0409$  for the common wave ( $n_1$ ) in relation to  $\gamma_{H_0 N}$

On the figures, the families of curves (6.6) are drawn with dotted lines. Next to each one is indicated the corresponding value of  $\nu$ . The group of thick lines represents the curves (6.7) which are constructed for the fixed values of  $\alpha_H$  in the interval  $\alpha_H = 0 + 0.3387$  and for the constant value  $\gamma = 0.9409$ . In all the calculations it is assumed that  $h^2 = 0.1$ . (In choosing the numerical values of the parameters we were guided by the comparison of calculations with

experimental results (5).) In order to reduce the size of the drawings, the families of curves (6.6) and (6.7) were drawn so that the corresponding values of  $\chi$  be taken into consideration corresponding to the direction of the arrows placed next to the curves. The direction of the arrows indicates the direction of "movement" of the wave front, first upwards from the beginning of the layer, then downwards from the point of wave reflection.

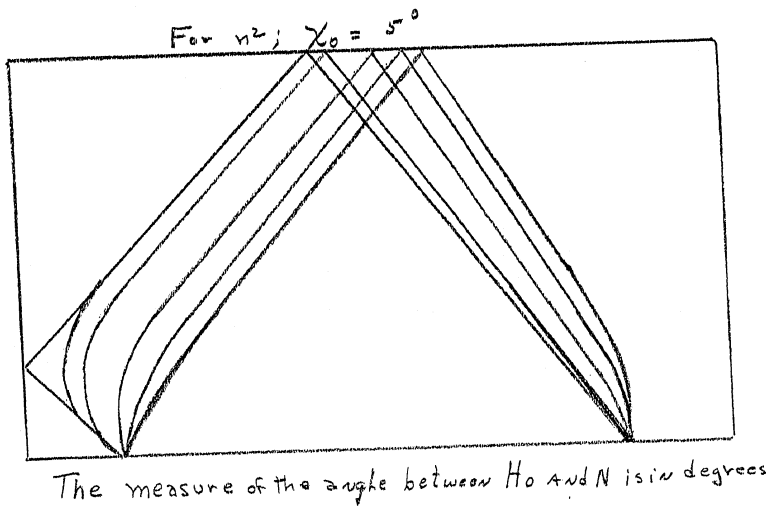


Figure 11. Same as in Figure 10, but for an uncommon wave ( $n_2$ )

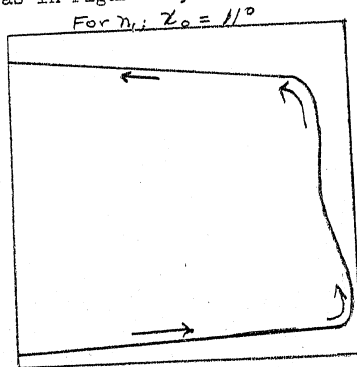


Figure 12. Curve of the relation between  $\chi$  and  $v$  with  $\chi_0 = 11^\circ$  for a common wave ( $n_1$ )

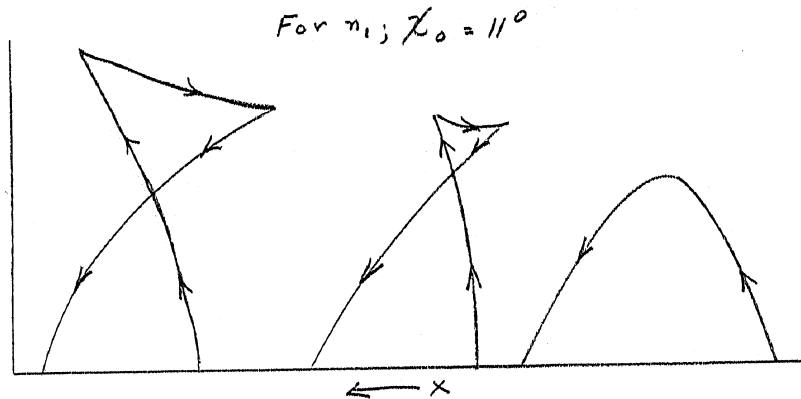


Figure 13. Trajectory of the normal to the front of an infinite flat monochromatic wave for various values of  $\psi H$

The points of intersection between the two families of curves on the drawings give us the totality of the values of  $\chi$  and of the corresponding values  $v$  and  $\gamma_{H_0 N}$  thus making a graphic presentation of  $\chi = \chi(v)$  and of the desired functions  $\alpha = \alpha(v)$  and  $\gamma = \gamma(v)$  possible. By way of illustration, Figure 12 shows the curve for just one case (for  $n_1$ ). The arrow next to the curve shows the direction of movement of the wave front in relation to the axis  $Z$ . (It should be said that the author mostly utilized tables of the values for the various functions, rather than graphs in all his calculations.)

An examination and an analysis of the function  $\chi(v)$  shows that its progress is asymmetrical.

This is explained by the asymmetrical nature of the progress of the ray in relation to  $H_0$  and leads us to the complex kinematics of the normal of the wave front in the layer (first noted by Zhekulin [3] as already indicated in the Introduction), and in particular to the fact that the turn of the wave front into the opposite direction (reflection of a flat monochromatic wave) happens not with those

values of  $v$  (and correspondingly of  $n$ ) where  $\gamma = 0$ , but rather with higher values of  $v$  (smaller than  $n$ ). The trajectory of the normal to the wave front (common and uncommon) traces a loop as it turns downwards. Figure 13 shows the results of a graphic presentation of the corresponding curves for a common wave ( $n_1$ ) and the values  $\chi_0 = 11^\circ$  with various values of  $\psi_H$ . Henceforth  $\psi_H$  will mean the angle between the X axis and the projection of the vector of the external magnetic field  $H_0$  onto the plane XY, i.e., the angle between the horizontal component of the magnetic vector and the plane of wave descent (see Figure 9). From Figure 13 we see that, when  $H_0$  lies on the plane perpendicular to the plane of descent, then the trajectory of the normal of the wave front is symmetrical in relation to the point of reflection. The curve with  $\psi_H = 0$ , or  $\pi$  has the biggest loop. We shall also see that the trajectory of the signal does not possess these peculiarities.

Thus we obtained all the data necessary to find the desired values of  $\alpha_1(v)$ ,  $\beta_1(v)$ ,  $\gamma_1(v)$ .

From the equations (6.1) ÷ (6.3) we obtain the following formulas which are convenient for the calculation:

$$\beta_1 = \frac{\sin \psi_0}{\sqrt{1+A^2}}, \quad (7.8)$$

$$\alpha_1 = A\gamma\beta_1 + \alpha \cos \psi_0, \quad \gamma_1 = -A\alpha\beta_1 + \gamma \cos \psi_0 \quad (7.9)$$

where

$$A = \frac{\alpha_H}{\beta_H} \gamma - \frac{\gamma_H}{\beta_H} \alpha.$$

For the totality of the  $v$  values and of the corresponding values  $\alpha$ ,  $\gamma$  and  $\psi_0$  (and also  $\gamma_{H_0N}$ ) obtained by the method shown, we have computed tables of the values of  $\alpha_1$ ,  $\beta_1$ ,  $\gamma_1$  obtained by means of formulas (7.8) and (7.9). For further manipulations it will be more convenient to use the values of the angular coefficients of the projections of the ray trajectory (vector  $U$ ) upon the coordinate planes. The corresponding angles with the X axis (on the plane XY), with the Z axis (on the plane XZ) and with the Y axis (in the plane YZ) are the results of these tables. Namely

$$\left. \begin{aligned} \psi_{xy} &= \text{Arc Tan } \frac{\beta_1}{\alpha_1} \\ \psi_{zy} &= \text{Arc Tan } \frac{\alpha_1}{\gamma_1} \\ \psi_{yz} &= \text{Arc Tan } \frac{\beta_1}{\gamma_1} \end{aligned} \right\} \quad (7.10)$$

The tables which we composed allowed us to analyze the trajectory of the ray and also to explain the peculiarities of the reflected wave. The pertinent results are treated in the following sections.

#### 7. STUDY OF THE RAY TRAJECTORY IN THE IONOSPHERE

In this section we bring the results of the calculation of the ray trajectory in the ionosphere which we conducted on the basis of a large number of graphs traced for various particular cases, and of tables composed with the help of the formulas cited above. In a number of drawings reflecting one part of these results, we show how the trajectories of the ray change in relation to the change of



various parameters.

All graph constructions were carried out for a linear layer. For layers of other shapes, for instance with a parabolic distribution of ionization, the effects here presented, as the analysis of the formulas will show, have an identical qualitative course and differ only in size.

Figures 14 and 15 show projections of the ray trajectories upon a horizontal plane (XY) for various values of  $\psi_H$  with  $\chi_0 = 5^\circ$ , respectively for common ( $n_1$ ) and uncommon ( $n_2$ ) waves. The direction of the ray motion (from the beginning to the end of the layer) is marked by the arrows on the drawing. We see that the ray, entering the layer, leaves the X axis, i.e., leaves the plane of descent. With low values of  $\psi_H$  the ray of a common wave travels into the opposite direction for part of its way in the deep regions of the layer (with high  $v$  values and low  $n$  values). Because of the asymmetric nature of the ray trajectory the ray comes out of the layer at a certain distance from the initial direction of the X axis. With  $\psi_H = 0$  (this is not shown on the drawing), the trajectory of the ray is flattened and the ray constantly remains in the plane of descent. The biggest deflection of the ray from the plane of descent occurs with a certain intermediate value of  $\psi_H$  in the interval of values  $\psi_H = 0 \pm \frac{\pi}{2}$ . With  $\psi_H = \frac{\pi}{2}$ , the progress of the ray is symmetrical in relation to the point of reflection, so that in the final analysis, the ray returns to the plane of descent. The ray progress of a common wave differs from that of an uncommon wave in that on the path of the ray's progress in the layer its sign of deviation from the plane of descent is different for each type of wave. The common wave deviates from the plane of descent in the



direction of the positive sign of the Y axis, while the uncommon wave deviates in the negative direction. As the ray returns from the layer, the uncommon wave deviates from the plane of descent into the direction of the positive side of the Y axis. However the degree of deviation of the ray from its initial direction has the same sign for both waves. It is higher for the common wave. Also, the trajectory of the ray of a common wave is somewhat more complex. It should be noted that all the drawings are in the right scale, so that their relative measures may serve as criterions for the effects observed. So, for instance, on Figure 14, for  $\psi_H = 27^\circ$ ,  $AB = 1/3 OA$ , which means that the ray, in this case, comes out of the layer on the side of the initial direction at a distance equal approximately to  $1/3$  of  $OA$  (the range of wave propagation).

For  $n_1; \chi_1 = 5^\circ$

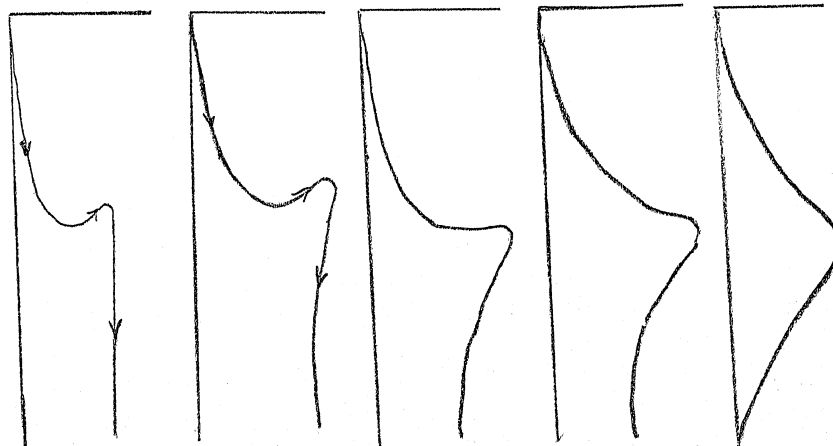


Figure 14. Projection of the ray trajectory (signal) upon a horizontal plane XY for various values of  $\psi_H$  when  $\chi_1 = 5^\circ$  for a common wave ( $n_1$ )

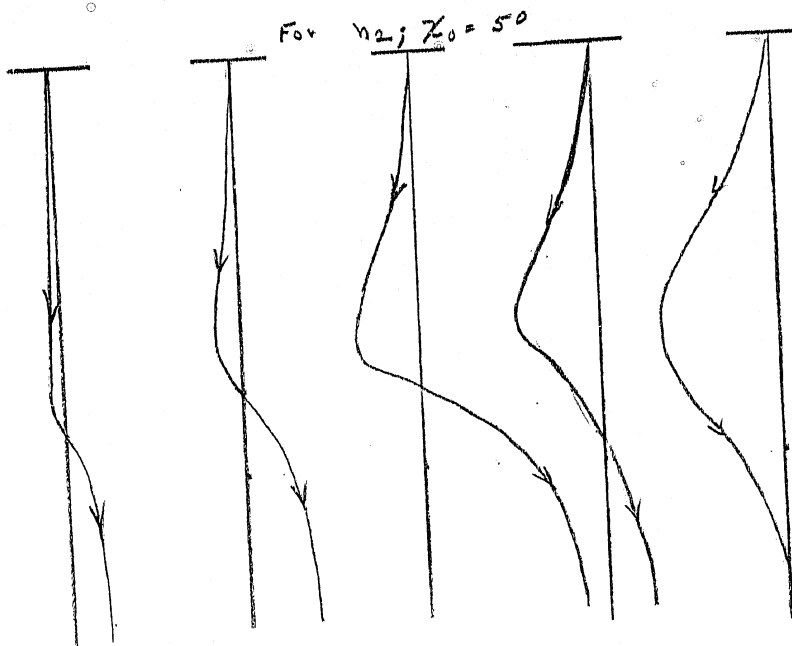


Figure 15. The same as in Figure 14, but for an uncommon wave ( $n_2$ )

Figure 16 shows the projections of the ray trajectory of a common wave (for  $n_1$ ) for various values of  $\psi_H$  and  $\chi_0 = 50^\circ$  at the plane of descent XZ, while Figure 17 shows the same for plane YZ perpendicular to the plane of descent. The figures clarify all the characteristic peculiarities of the ray's progress. One should note a new important condition which derives from Figure 16. From it we see that with a given angle  $\chi_0$  (angle of descent of the wave upon the layer) the propagation range of the ray for a common wave (distance OX) strongly depends from the angle  $\psi_H$ .

Figure 17 clearly shows the side deviation of the ray OY which we mentioned before. Figure 18 shows the respective projections of the ray trajectory for an uncommon wave (for  $n_2$ ). From the figures we see the peculiarities of the ray trajectory which interest us.

For  $n_2; \chi_0 = 5^\circ$

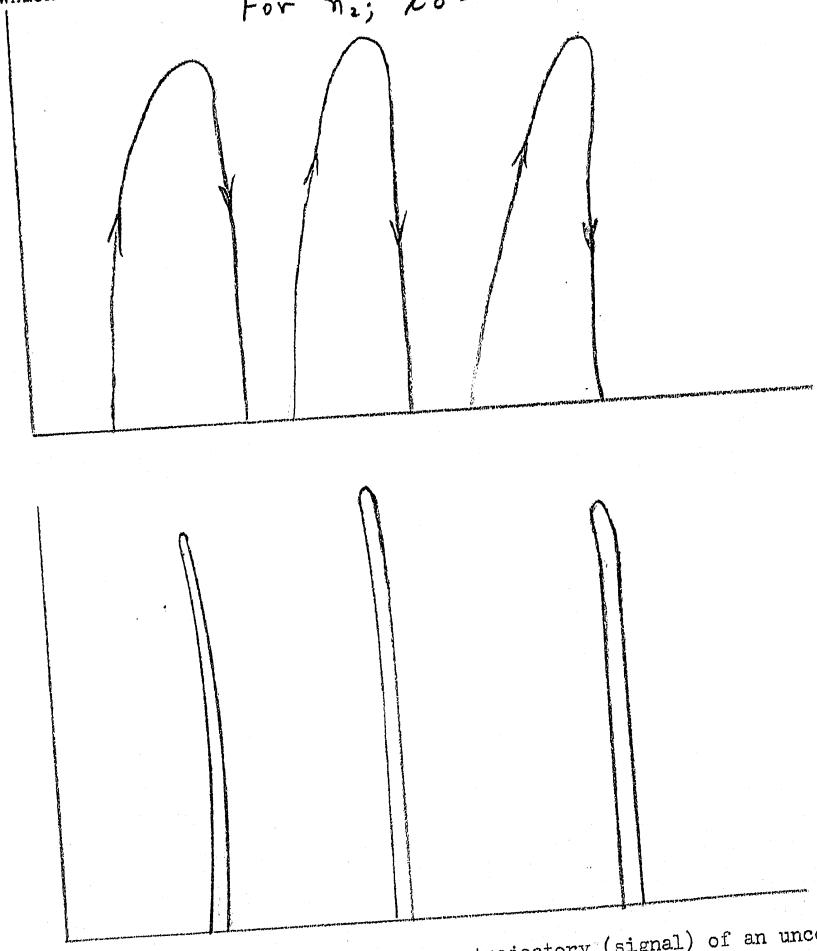


Figure 18. Projections of the ray trajectory (signal) of an uncommon wave ( $n_2$ ) upon the plane of descent XZ (upper part of the figure) and upon the plane YZ (lower part of the figure), for various values of  $\psi_H$  with  $\chi_0 = 5^\circ$

The preceding figures characterized the trajectory of the ray in the layer for a fixed value of the angle of descent  $\chi_0$ . However it is interesting to examine the relation between these effects and  $\chi_0$ . Figures 19 and 20 show a few results of such an analysis. Figure 19 shows that with an increase of the angle of descent  $\chi_0$  the corresponding deviation of the ray  $\frac{AB}{OA}$  from the plane of descent decreases and tends towards zero. In the region of low values of  $\chi_0$  the corresponding deviation is large. Here it has its maximum. However, as the limit passage shows, in the region of low values of  $\chi_0$  the size of AB swiftly decreases with a decrease of  $\chi_0$  and becomes equal to zero with  $\chi_0 = 0$  (see Figure 20). With a vertical descent ( $\chi_0 = 0$ ) the ray at first deviates considerably from the plane of descent. Its trajectory lies on the plane (ZH<sub>0</sub>). On the way back, the reflected wave has the same trajectory, so that the ray leaves the layer at the same point where it entered. The corresponding projections of the ray trajectory are shown in Figure 20.

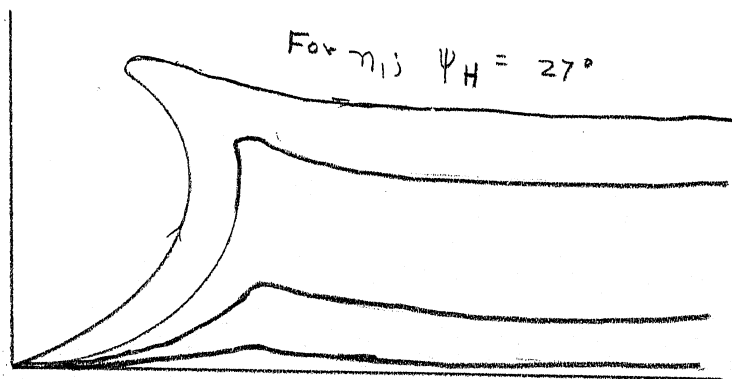


Figure 19. Projections of the ray trajectory (signal) of a common wave ( $n_1$ ) upon the plane XY for various values of the angle of

descent  $\chi_0$  with  $\psi_H = 27^\circ$

For  $n_1$ ;  $\psi_H = 27^\circ$

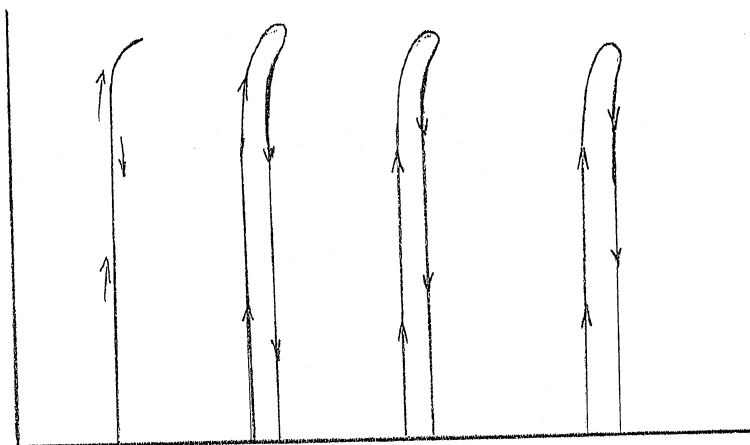
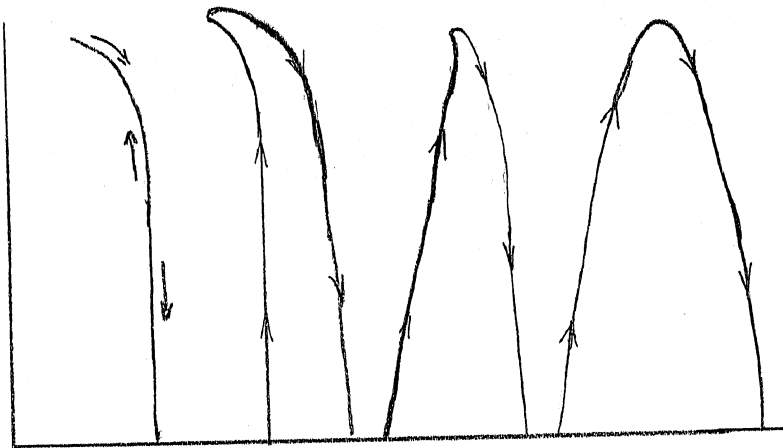


Figure 20. Projections of the ray trajectory (signal) of a common wave ( $n_1$ ) upon the plane of descent XZ (upper part of the figure) and upon the plane YZ (lower part of the figure) for various values of  $\psi$  with  $\psi_H = 27^\circ$

Figure 21 gives the axonometric presentation of the ray trajectory of a common wave in the ionosphere. Here its peculiarities are clearly visible.

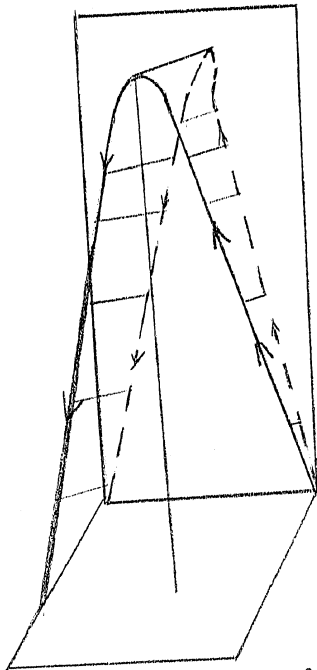


Figure 21. Axonometric presentation of the ray trajectory (signal) of a common wave in the ionosphere

From this analysis of the ray trajectory in the ionosphere it is absolutely clear that the wave reflected from it does not have a spherical shape (if the descending wave is spherical) and that in the horizontal plane XY (on the surface of the earth) the shape of the wave front is not circular. This happens because the receiving point gets not that segment of the wave that has issued from the radiation point and whose normal passed through the receiving point, but another segment of the wave whose normal formed a certain angle with this initial direction.

The direction of the wave front at the receiving point which here, because of the isotropic nature of the medium coincides with the direction of the group speed vector and with Pointing's vector  $\vec{S}$ , forms a certain angle with the line connecting the receiving point with the point of radiation.

The corresponding topographic picture on the plane XY for a common wave with  $\chi_0 = 5^\circ$  is shown on Figure 22. Here the point O indicates the circular shape of the descending wave front. We see how certain segments of the wave front (1 - 5) are transferred on their way from the entrance into the layer to the exit, respectively, to the points (1' - 5'). The normals of these segments of the wave front (with  $\psi_H \neq$  and  $\psi_H \neq \frac{\pi}{2}$ ) a sharp angle with the true direction -- the line connecting points (0.1'), (0.2'), (0.3'), (0.4'), (0.5').

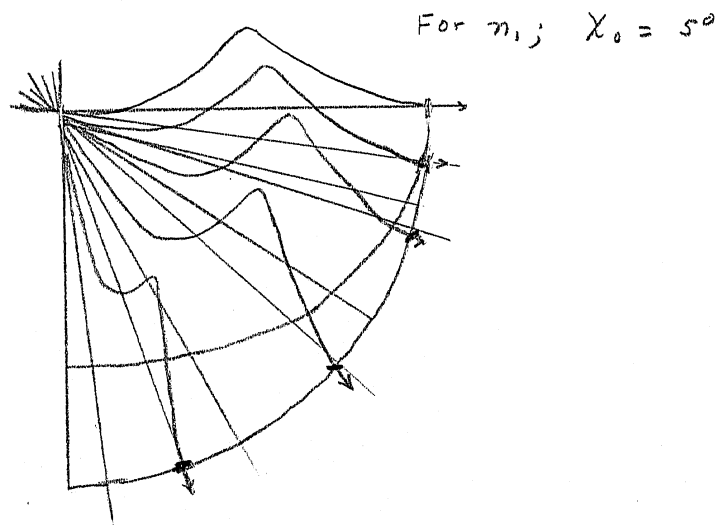


Figure 22. Family of projections of ray trajectories (signals) of a common wave ( $n_1$ ) upon a horizontal plane (XY) in relation to  $\psi_H$



In the figure, at points 1' - 5' the true direction is indicated with a thin arrow while the wave front is indicated with a black arrow.

Figure 22 proves that in the plane XY the reflected wave has an elliptical shape.

As a result of the plottings, part of which are shown in the above figures, it was possible to calculate the relation between the angle (between the direction of the normal of the reflected wave front and the line connecting the receiving point with the point of observation in the horizontal plane) and the angle both for common and uncommon waves ( $n_1$ ) and ( $n_2$ ) respectively. (See Figure 23.) The sign of the angle is positive with a clockwise reading.

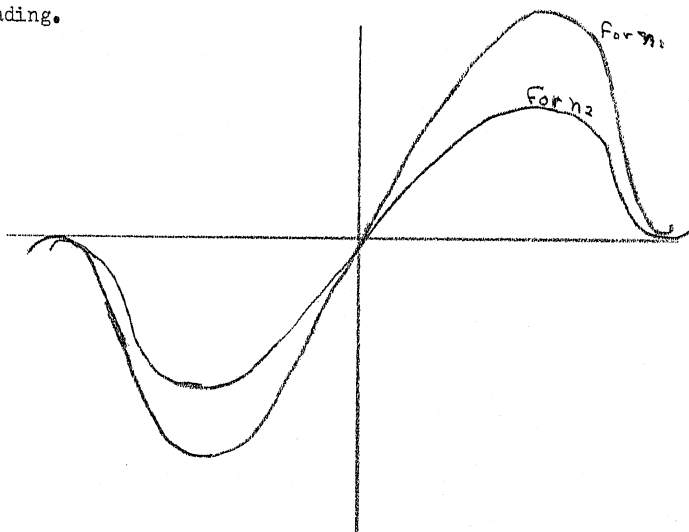


Figure 23. Relation of the angle between the direction of the normal to the front of a reflected wave on a horizontal plane and the true direction, to the angle  $\psi_H$  for a common wave (thin line), and  $\psi_0$  an uncommon wave (thick line) with a descent angle of  $5^\circ$ .

One must bear in mind that the precision of the data obtained is subject to the precision of graph plotting and therefore there are quantitative errors of the order of a few percent. The curve  $\alpha(\psi_H)$  is built for the interval  $-\frac{\pi}{2} + \frac{\pi}{2}$ . An analysis shows that it is not symmetrical in relation to the points  $\psi_H = \pm \frac{\pi}{2}$ . This circumstance and other peculiarities of the ray trajectory are made comprehensible by basic physical considerations, to wit that in a magnetically active medium the principle of reciprocity is nonexistent. Phenomena occur in different ways depending on whether the waves propagate along or against the direction of the external magnetic field.

#### 8. BASIC CONCLUSIONS

In the preceding paragraphs we have shown the results of the calculation of the propagation of electromagnetic waves in a magnetically active, nonhomogeneous medium. First we studied and gave more precision to the general properties of the monochromatic wave in a homogeneous medium, and then we did the same with the properties of the quasi-monochromatic group of waves (signal). In the case of the ~~medium~~ nonhomogeneous medium in the direction of the Z axis we made certain indispensable generalizations in the approximation of geometrical optics. In the latter part of the work we calculated the trajectory of the ray in a nonhomogeneous medium of the ionosphere type, which is characteristic in that in the direction of the Z axis the refraction exponent of the medium evenly decreases from its value equal to one at the beginning of the layer. This leads to a deviation of the ray in the direction of Z and to the reflection of the wave descending on the layer. We examined the relation between the character of the trajectory of the reflected ray and the various

parameters. We also examined the shape of the reflected wave.

This work allows us to make certain new conclusions:

(1) In a magnetically active medium, as a consequence of the splitting of the linearly polarized wave into two elliptically polarized waves which propagate in it at different speeds, the position of Pointing's vector in the space of each wave is not constant: Pointing's vector traces a cone in each point. This cone touches the normal to the wave front. Pointing's vector circles the surface of the cone twice during each period. The basis of this cone is a flat curve of elliptical shape. The line traced from the apex of the cone through the center of its base lies on the plane  $H_0N$ . The direction of this line coincides with the direction of Pointing's vector  $\bar{S}$  averaged in time.

(2) It is absolutely clear that for a full and serious analysis of the question it is physically correct to examine the propagation of the quasi-monochromatic group of waves. This leads to the necessity of studying the integral of Fourier.

The analysis of Fourier's integral allowed us to calculate the direction and value of the vector  $U$  of group speed which characterizes the propagation of the quasi-monochromatic group of waves.

A comparison of the vector  $U$  with the vector of Pointing  $\bar{S}$  averaged in time, made by way of direct calculation, showed that both vectors are collinear.

The vector  $U$  is characterized by the following properties:

(a) It is placed in the plane containing the normal to the wave front  $N$  and the vector of the external magnetic field  $H_0$ .

(b) The formula determining the value of the group speed  $U$  differs from the formula determining the value of group speed  $U_0$  when  $H_0 = 0$ .

(c) The proportion  $\frac{U_0}{U}$  is equal to the cosine of the angle between the vectors  $U$  and  $N$  at a given point of the medium.

(3) A direct generalization of the results obtained for the case of a nonhomogeneous stratified medium (nonhomogeneity in the direction of the  $Z$  axis) gave the usual formula for the calculation of the time of the group retardation of the signal. For the reflection of the ray from the ionosphere we drew a condition not coinciding with the corresponding condition for the isotropic medium which must serve (instead of the formulas commonly used) for the determination of the ionization degree of that region of the layer in which a wave of a given frequency reflects upon its slanted descent on the layer.

(4) The formulas obtained and the general properties of the ray determined through the analysis of these formulas allowed us, by way of a combination of graphs and direct calculations, to establish a series of tables of the values of angular coefficients of the ray trajectory. These tables are gathered for a significant diapason of transformation of individual parameters. This allowed us to follow the limit passages of the ray trajectory.

The choice of the diapason of transformation of the individual parameters was dictated by the necessity of a closer comparison with experimental results.

The following properties of the ray trajectory have been established:

(a) The ray trajectory is a space non-flat curve. The rays issue from the plane of descent. Exceptional is the case when the vector of the external magnetic field lies in the plane of descent. In this case the ray trajectory remains in the same plane.

(b) The ray trajectory is not symmetrical in relation to the point of reflection and the ray does not return to the plane of descent. In a horizontal plane it does not leave the layer along the initial direction (projection of the normal at the point of descent to the layer), but to one side of it. Moreover, at this point the direction of the wave normal coincides with its direction to the point of issue.

An exception is the case when the vector of the external magnetic field lies in the plane perpendicular to the plane of descent. In this case the ray trajectory is symmetrical in relation to the reflection point and the ray returns to the plane of descent -- comes out of the medium in the initial direction.

(c) The relative deviation of the ray in the horizontal plane has the same sign for the common and uncommon waves and differs only in size -- it is higher for a common wave. The trajectories of the common and the uncommon waves also differ in many details. So, for instance, in the cases examined, the ray of a common wave propagates in certain parts of the layer in the opposite direction.

(d) The properties of the ray indicated in (a), (b) and (c) lead to the fact that the reflected wave does not keep the spherical shape of the descending wave -- in the horizontal plane the wave front has an elliptical shape.

(e) The direction of the incoming ray at the receiving point does not coincide with the direction of the line which connects it with the radiation point. It forms with it a certain angle  $\alpha$  the sign and magnitude of which depends on the angle between the projection of the vector of the external magnetic field and the plane of descent. As the distance between the points of radiation and reception grows, i.e., as the angle of descent onto the layer increases, the magnitude of this angle gradually decreases and tends towards zero. The magnitude of this angle reaches 10 and in certain cases 20 and more degrees with comparatively small distances from the radiator.

Upon vertical descent onto the layer, the ray at first propagates on the plane  $H_0N$ . It returns along the same trajectory and leaves the layer at the same point.

(5) The conclusions mentioned above derive from a theoretical analysis of the ray trajectory in the ionosphere. They indicate that for practical calculations and for the processing of data on the ionosphere it is indispensable:

(a) To take into consideration the relation between the range of ray propagation, especially for close distances, and  $\psi_H$  and other parameters which at the present time are not considered.

(b) Strictly speaking it is necessary, while calculating the degree of ionization of the layer at the point of reflection with a slanted descent onto the layer, to take advantage of the condition (formula (5.21)), which is correct for the ionosphere if we consider its state of anisotropy.



(c) When finding the direction of the ray, especially for close distances, it is necessary to take into consideration the correction made above (see Figure 23). This correction is the consequence of the anisotropic properties of the ionosphere. This is an "error in direction finding" which results from the nature of things.

This increasing precision may lead in certain cases, as may be seen from the numerical examples mentioned above to substantial quantitative changes.

Physics Institute imeni P. N. Lebedev  
Academy of Sciences USSR

#### QUOTED LITERATURE

- (1) Gans R., Ann. d. Physik, 47, 709 (1915)
- (2) Al'pert Ya. L., Propagation of Radio Waves in the Ionosphere.  
Gostekhizdat, 1947
- (3) Zhekulin L. A., Vestnik elektrotehniki (Electrotechnical News) 2, 63 (1930); Jahrbuch der Drahtl. Telegr. u. Teleph., 36, 172 (1930)
- (4) Booker H., Phil. Trans. Roy. Soc., 237, 411 (1938)
- (5) Al'pert Ya L., DAN USSR, 53, 703 (1947); Izvestiya AN CCR (News of the Academy of Sciences), Physics Series, 12, 2, 267 (1948)
- (6) Goubau G., Hochfr. und Elektroakustik, 44, 17, 930 (1934)
- (7) Rytov S. M., ZhETF, 17, 930 (1947)